

See discussions, stats, and author profiles for this publication at: <https://www.researchgate.net/publication/236908990>

Quantum Chemical Study of the Reactions between Pd⁺/Pt⁺ and H₂O/H₂S

ARTICLE in CHEMISTRY - A EUROPEAN JOURNAL · MAY 2013

Impact Factor: 5.73 · DOI: 10.1002/chem.201300222 · Source: PubMed

READS

34

5 AUTHORS, INCLUDING:



Jon M Matxain

Universidad del País Vasco / Euskal Herriko...

83 PUBLICATIONS 1,422 CITATIONS

SEE PROFILE



Fernando Ruipérez

Universidad del País Vasco / Euskal Herriko...

52 PUBLICATIONS 420 CITATIONS

SEE PROFILE



P. B. Armentrout

University of Utah

493 PUBLICATIONS 20,560 CITATIONS

SEE PROFILE

Quantum Chemical Study of the Reactions between Pd⁺/Pt⁺ and H₂O/H₂S

Oier Lakuntza,^{*,[a]} Jon M. Matxain,^[a] Fernando Ruipérez,^[a] Jesus M. Ugalde,^[a] and Peter B. Armentrout^[b]

Abstract: The study of the reactions of water and hydrogen sulfide with palladium and platinum cations has been completed in this work, in both low- and high-spin states. Our calculations predict that only the formation of platinum sulfide is exothermic (in both spin states), whereas for the remaining species the oxides and sulfides are found

to be more reactive than their corresponding bare metal cations. An in-depth analysis of the reaction paths

Keywords: computer chemistry • density functional calculations • palladium • platinum • transition metals

leading to metal oxide and sulfide species is given, including various minima, and several important transition states. All results have been compared with existing experimental and theoretical data, and earlier works covering the reaction of nickel cation with water and hydrogen sulfide to observe the trends for the group 10 transition metals.

Introduction

The study of the reactivity of bare transition-metal cations in the gas phase is of utmost importance given the role they play in a variety of chemical processes, including the crucial and challenging σ -activation process.^[1–16]

Among these studies, the reactions between transition-metal cations and water have been extensively studied from the pioneering state-specific studies of Armentrout et al., who laid out most of the main issues,^[17–19] to the recent measurements by Bohme et al., who have compiled their results in a recent report.^[20]

Additionally, quantum chemistry mechanistic studies performed for the early,^[21–23] middle,^[24,25] and late^[26] first-row transition metals agreed with the experimental evidence,^[20] which showed that whereas for early first-row transition metals their bare cations are more reactive than their oxides, the opposite is the case for the late transition-metal cations.^[27] Moreover, in most of these reactions there is at least one spin-crossing, and thus, depending on the spin state of the reactants, the efficiency of the reaction varies drastically.^[17,19]

The reactions with water are important in themselves because water is ubiquitous in most reaction environments as well as in many man-made devices, as a background impuri-

ty and, consequently, it constitutes a likely reactive target for transition metal cations. Furthermore, in a number of cases the intermediates occurring along the reaction path constitute themselves as very interesting species with unique chemical properties.

Thus, Schwarz et al. found that, for the reaction of nickel cation and water,^[28] the first intermediate of the reaction, namely, the nickel cation water complex, is inactive towards the activation of the C–H bond of methane, but the central intermediate, namely, the nickel hydrido hydroxy cation, does activate methane under thermal conditions according to the following Equation (1).




Theoretical calculations suggested that the HNiOH^+ can isomerize to the nickel cation water complex,^[24] and thus, depending on the energy barrier of this process, the activation of methane might take place. In this vein, Schwarz, Baik, and co-workers^[29] have recently unveiled that the hydroxyl ligand of the previously mentioned HNiOH^+ intermediate behaves as a redox non-innocent ligand, yielding its higher energy quartet state ($^4\text{A}''$) not connected with its doublet ground state ($^2\text{A}''$) by a single electron spin-flip, inhibiting in this way the intersystem crossing. Therefore, the quartet spin state can be long-lived enough to undergo reactions with CH_4 and also with the O_2 molecule.^[30] On the other hand, the doublet spin state undergoes rapid rearrangement to the nonreactive C_{2v} symmetric $\text{Ni}^+\cdots\text{OH}_2$ complex, as demonstrated by using simple quantum molecular dynamics calculations.^[12]

In related previous work,^[12] we studied the reaction between Ni^+ and H_2S to understand the influence of changing the oxygen to sulfur. As in the case of HNiOH^+ , whereas in the doublet state there is a negligible barrier associated with the $\text{HNiSH}^+/\text{NiSH}_2^+$ isomerization, in the quartet state, this

[a] Dr. O. Lakuntza, Dr. J. M. Matxain, Dr. F. Ruipérez,
Prof. Dr. J. M. Ugalde
Kimika Fakultatea, Euskal Herriko Unibertsitatea (UPV/EHU)
and Donostia International Physics Center (DIPC)
P.K. 1072, 20018 Donostia, Euskadi (Spain)
Fax: (+34) 943015270
E-mail: olakuntza@ehu.es

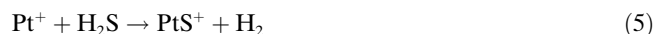
[b] Prof. P. B. Armentrout
Department of Chemistry, University of Utah
314 S. 1400 E. Rm 2020, Salt Lake City UT 84112 (USA)

 Supporting information for this article is available on the WWW under <http://dx.doi.org/10.1002/chem.201300222>.

energy barrier is much larger. However, in contrast to HNiOH^+ , the quartet state of HNiSH^+ is coupled to its almost energy-degenerate doublet state by a single spin-flip, so that once the latter is formed, it would rearrange rapidly to the much more stable NiSH_2^+ , which would not activate methane.

Although a great deal has been elucidated regarding the mechanism of the reactions between first-row transition-metal cations with water and hydrogen sulfide, much less is known about the reactions of second- and third-row transition-metal cations^[31] and of heavier elements as well.^[32] Recall that for reactions involving these elements, relativistic effects may play a significant role. Indeed, relativistic effects dominate the chemistry of metal cations with atomic numbers greater than about 50,^[33] and the differences in the chemistry of the second- and third-row cations can be largely explained considering the lanthanide contraction. Consequently, it is expected that in the group of nickel, not only for platinum, but also for palladium, the relativistic effects should play an important role in the reactions of these metals or their cations with small molecules.^[34–37]

In this work, we have studied theoretically the potential energy surfaces of the Equations (2)–(5) between Pd^+/Pt^+ cations and $\text{H}_2\text{O}/\text{H}_2\text{S}$, both in their low-spin doublet and high-spin quartet states.



Additionally, we have compared the calculated potential energy surfaces with the already studied reactions of the nickel cation with H_2O ^[24] and H_2S ^[12] to investigate trends in the reactivity along the group 10 metal cations. Special attention will be devoted to the central intermediates HMXH^+ ($\text{M}=\text{Pd}, \text{Pt}$; $\text{X}=\text{O}, \text{S}$) of these reactions, for the analogous HNiOH^+ has been found to activate methane under mild conditions.^[28]

Finally, it is worth mentioning that since we will be dealing with two different spin potential energy surfaces (doublet and quartet), intersystem crossing between these surfaces might take place. Wherever such crossings occur on the potential energy surfaces, we have characterized the minimum energy crossing point (MECP) by optimizing the energy of the crossing point on the seam line at which the doublet and quartet adiabatic surfaces intersect.^[38]

Methods

All the structure optimizations have been carried out with the Gaussian 09^[39] and ADF^[40] suites of programs. The structures shown in this paper were optimized by using the hybrid generalized B3LYP^[41–43] gradi-

ent approximate functional within density functional theory.^[44,45] In these calculations, we have used a relativistic effective core potential (RECP) to replace the 28 and 60 core electrons of palladium and platinum, respectively. For their valence electrons we have used a cc-pVTZ basis set.^[46,47] For the sulfur, oxygen, and hydrogen, the 6-311++G(2df,2p) basis set of Pople and co-workers^[48] was used. We have denoted this combined RECP, for the core electrons, and Gaussian-type basis set function, for the valence electrons, with cc-pVTZ. Then, harmonic vibrational frequencies were calculated by analytical differentiation of gradients, to determine whether the structures found were true minima or high-order stationary points, and to extract zero-point energies and Gibbs free energy contributions.

Additionally, all these structures were also optimized with the PBE0 generalized gradient functional^[49] and an all-electron basis set, namely, the triple- ζ quality TZ2P exponential-type basis set. In these calculations relativistic corrections were accounted for by the Zeroth Order Regular Approximation (ZORA).^[50,51] We found no significant difference with respect to the B3LYP/cc-pVTZ optimum structures, in accordance with our earlier gained experience^[52] that suggests that the hybrid B3LYP functional^[41–43] with the cc-pVTZ basis set is a reliable choice for optimization and frequency calculations for the type of systems studied in this work.

Finally, to improve the relative energies of the characterized structures, CCSD(T)^[53,54] single-point calculations were carried out at the geometries optimized at the B3LYP/cc-pVTZ level of theory.

The accurate estimation of the MECs represents a more challenging problem because of the highly multiconfigurational nature of the wave functions of the systems at these nonstationary nuclear configurations. We have characterized the reported MECs at the CASPT2 level of theory, in which the active space in the CASSCF step is made from distributing 17 valence electrons in 12 molecular orbitals. We have employed the all-electron ANO-RCC basis sets of quadruple- ζ quality, developed by Roos and co-workers.^[55–57] All these calculations have been performed by using the MOLCAS 7.4 suite of programs.^[58]

Results and Discussion

Excitation energies: In the reactions studied, there are four doublet-quartet splitting energy gaps that are exceptionally important, thus we describe them more exhaustively. These four are the bare metal cations M^+ , $\text{M}^+ \cdots \text{XH}_2$, HMXH^+ , and MX^+ ($\text{M}=\text{Pd}, \text{Pt}$ $\text{X}=\text{O}, \text{S}$) moieties. Excitation energies for these systems and for their analogous structures of the $[\text{Ni}, \text{O}, \text{H}_2]^+$ and $[\text{Ni}, \text{S}, \text{H}_2]^+$ systems are shown in Table 1. Recall that the spin-orbit coupled states have not been considered and only spin-orbit average term energies are shown.

Inspection of the data shown in Table 1 reveals a number of remarkable trends. Thus, it is observed that the known increase of the quartet/doublet energy gap from Ni^+ to Pd^+ , and then the abrupt decrease for Pt^+ , as a consequence of the lanthanide contraction of the 6s orbital, is well captured by all three levels of theory used in the present research.

The remaining excitation energies are also satisfactorily described by using the two density functional methods, B3LYP and PBE0(ZORA), as compared to CCSD(T). In particular, it is worth noting the remarkable performance found for the excitation energies of the intermediate HMXH^+ and for the MX^+ diatoms, in which PBE0(ZORA) appears to be slightly superior to B3LYP. This emphasizes the importance of the relativistic effects for these species having heavy elements. Recall that we have chosen B3LYP

Table 1. CCSD(T)//B3LYP, B3LYP, and PBE0(ZORA) relative energies [eV] for the quartet state M^+ (Δ_1), $M\cdots XH_2^+$ (Δ_2) and $HMXH^+$ (Δ_3) relative to their doublet ground state, and that of the doublet MX^+ relative to its quartet ground state (Δ_4).

	Method	Δ_1	Δ_2	Δ_3	Δ_4
[Ni,O,H ₂] ^[24]	CCSD(T)//B3LYP	1.27	1.55	0.76	0.61
	B3LYP	1.21	1.57	0.41	0.54
	experimental ^[67]	1.08			
[Ni,S,H ₂] ^[112]	CCSD(T)//B3LYP		1.69	−0.01	0.23
	B3LYP		1.74	−0.11	0.20
[Pd,O,H ₂] ⁺	CCSD(T)//B3LYP	2.91	3.19	1.41	0.49
	B3LYP	2.87	3.13	1.22	0.40
	PBE0(ZORA)	3.53	3.56	1.41	0.41
	experimental ^[67]	3.19			
[Pd,S,H ₂] ⁺	CCSD(T)//B3LYP		3.40	1.71	0.29
	B3LYP		3.21	1.51	0.23
	PBE0(ZORA)		3.61	1.71	0.28
[Pt,O,H ₂] ⁺	CCSD(T)//B3LYP	0.70	1.23	1.51	0.31
	B3LYP	0.75	1.30	1.32	0.25
	PBE0(ZORA)	0.99	1.34	1.45	0.27
	experimental ^[67]	0.76			
[Pt,S,H ₂] ⁺	CCSD(T)//B3LYP		1.87	1.81	0.21
	B3LYP		1.89	1.65	0.15
	PBE0(ZORA)		2.06	1.83	0.18

to treat relativistic effects through a relativistic effective core potential whereas in PBE0 we use an all-electron basis set and relativistic effects are treated by ZORA.

For the entrance ion molecule, substitution of oxygen by sulfur widens the quartet/doublet energy gap, Δ_2 . This trend is more pronounced for the platinum than for the nickel and palladium.

In contrast to the $[Ni,X,H_2]^+$ systems, the $HMXH^+$ intermediates of palladium and platinum have larger quartet/doublet energy gap for S-containing compounds than for O-containing compounds. Notice that in the case of Ni, for the S-containing intermediate, the quartet/doublet energy gap is slightly in favor of the quartet state by 0.01 eV,^[12] whereas for the O-containing intermediate, the quartet/doublet energy gap is 0.76 eV, with the doublet being the ground spin state.^[24]

Finally, we have examined the metal oxide and sulfide MX^+ diatomic cations. All the quartet/doublet energy gaps of these cation molecules (except that of the NiS^+) correspond to the splitting energies between the $^4\Sigma$ and $^2\Sigma$ states. Notice that for all three transition metals, the exchange of oxygen by sulfur lowers the quartet/doublet energy gap.

Reaction mechanisms: Tables 1–4 of the Supporting Information show the relative energies with respect to the reactants of the Equations (2)–(5) for the low- and high-spin states at the CCSD(T)//B3LYP, B3LYP, and PBE0(ZORA) levels of theory. Since all three methods yield consistent numbers, we shall relay our discussion on the CCSD(T)//B3LYP level of theory results. Figures 1 and 2 show the CCSD(T)//B3LYP relative energy profiles of the corresponding characterized reactions paths of Equations (2)–(5). The xyz coordinates of all the structures alluded to in Figures 1 and 2 can be found in the Table 5 of the Supporting Information.

The reaction mechanisms for all four cases can be described as two sequential hydrogen atom shifts from either the oxygen or sulfur atoms over to the metal atom, followed by a subsequent release of the molecular hydrogen formed in the coordination sphere of the transition metal. However, a closer inspection of Figures 1 and 2 and Table 5 of the Supporting Information reveals a number of remarkable differences worth pointing out.

Thus, we have found that for palladium, the formation of molecular hydrogen occurs simultaneously with the transfer of the second hydrogen atom, yielding the corresponding $H_2\cdots PdX^+$ ($X = O, S$) dihydrogen complex. However, for platinum, the transfer of the second hydrogen yields a stable Kubas-like dihydride complex. Subsequently, this complex evolves towards the $H_2\cdots PtX^+$ ($X = O, S$) dihydrogen complex through transition state TS3 (see Figure 2) and, finally, the hydrogen molecule is released from this complex without an activation barrier.

The spin state of the ground state of the reactants of all four Equations (2)–(5) is the doublet state, and the spin state of the ground state of the products is the quartet state. This is the typical case for the two-state reactivity scenario^[59] involving the mentioned doublet and quartet potential energy surfaces. Inspection of Figure 1 and 2 reveals that there is only one crossing along their corresponding reaction paths. However, whereas for the reactions of Pd^+ such crossings take place between TS2 and the $H_2\cdots PdX^+$ ($X = O, S$) complex, during the shift of the second hydrogen atom over to the Pd center, for the reactions involving Pt^+ the crossings occur at a later stage between TS3 and the $H_2\cdots PtX^+$ ($X = O, S$) complex, during the formation of the hydrogen molecule from the two hydrido hydrogen atoms of the Pt center.

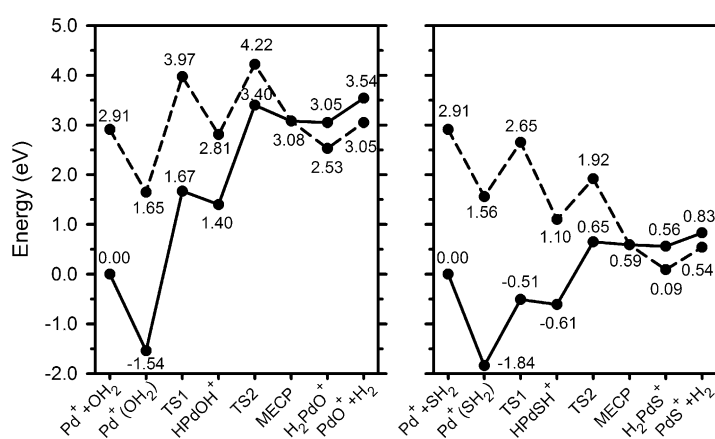


Figure 1. CCSD(T)//B3LYP potential energy surfaces following the $Pd^+ + OH_2 \rightarrow PdO^+ + H_2$, left panel, and $Pd^+ + SH_2 \rightarrow PdS^+ + H_2$, right panel, reaction paths. Relative energies with respect to the reactants are in eV. Solid lines correspond to the doublet spin surfaces and dashed ones to the quartet spin surfaces.

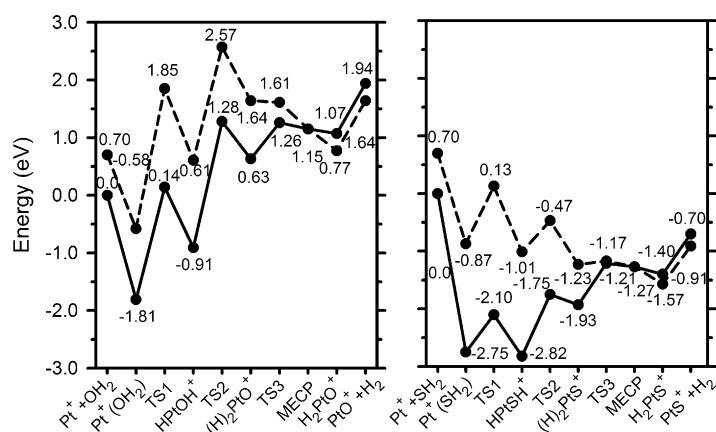


Figure 2. CCSD(T)//B3LYP potential energy surfaces following the Pt⁺ + OH₂ → PtOH⁺ → PtO⁺ + H₂, left panel, and Pt⁺ + SH₂ → PtSH⁺ → PtS⁺ + H₂, right panel, reaction paths. Relative energies with respect to the reactants are in eV. Solid lines correspond to the doublet spin surfaces and dashed ones to the quartet spin surfaces.

The reactions of both Pd⁺ and Pt⁺ with OH₂ are endothermic on both the doublet and the quartet potential energy surfaces. The reaction of Pd⁺ with SH₂ is endothermic on the doublet surface, but it is exothermic when Pd⁺ is prepared in its excited quartet state, as shown in the right panel of Figure 1. Finally, it is worth noticing that the reaction of Pt⁺ with SH₂ is exothermic on both spin potential energy surfaces. Consequently, our calculations predict that whereas H₂ could desulfurate exothermically PdS⁺ to yield Pd⁺ and SH₂, Pt⁺ could dehydrogenate SH₂ to yield PtS⁺ and H₂ exothermically. The deoxygenation of PdO⁺ by H₂ is exothermic but it is predicted to be impeded by sizeable kinetic barrier of 0.35 eV. The deoxygenation of PtO⁺ by H₂ is also exothermic, but it is not kinetically impeded, provided an efficient spin crossover at the MECP (see left panels of Figures 1 and 2).

These potential energy surfaces also provide some insight into the experimental observations available in the literature for these reactions. To date, no studies of the reactions of H₂S have been performed, but Bohme and co-workers have examined the room temperature reactions of Ni⁺, Pd⁺, and Pt⁺ with D₂O in a flow tube at a He pressure of 0.35 Torr.^[20] In all three cases, the only primary product formed is the M⁺(D₂O) complex, which is formed in a termolecular process at the high He pressure. These observations are consistent with the barrierless interaction potential of M⁺ with H₂O and the endothermic nature of the potential energy surfaces for formation of MO⁺ + H₂, as shown here in Figures 1 and 2 and previously for M⁺ = Ni⁺.^[26] Furthermore, the experimental rates of reaction are 1.7, 0.7, and 4.7 × 10⁻¹² cm³ molecule⁻¹ s⁻¹, respectively. Because the rates of formation of the M⁺(D₂O) complexes are determined in part by the lifetime of the M⁺(D₂O) complex formed by association of M⁺ with D₂O. This lifetime depends on the depth of the M⁺(D₂O) potential well and the distribution of vibrational frequencies. We note that the well depth at 0 K for Ni⁺(H₂O) has been measured as (1.87 ± 0.03) eV,^[60] and

those for Pd⁺(H₂O) and Pt⁺(H₂O) are calculated here as 1.54 and 1.81 eV, respectively. Thus the low rate of Pd⁺(D₂O) formation can be directly attributed to smaller dissociation energy, leading to a shorter lifetime. For Ni⁺ and Pt⁺, which have comparable well depths, the relative rates of formation can probably be attributed to the lower frequencies associated with the heavier metal, such that the density of states of the Pt⁺(D₂O) complex is higher than that of Ni⁺(D₂O), which will increase the lifetime of the former intermediate compared with that of the latter, in agreement with experimental results.

Electronic structure of HMXH⁺ (M = Pd, Pt; X = O, S): The T1-diagnostic^[61] is used to measure the contribution of the singly excited configurations and serves as an indicator for near degeneracy effects.^[62] A T1-diagnostic value larger than the recommended threshold^[63] of T1 = 0.04, indicates that the electronic state is multiconfigurational in nature. Consequently, single-reference methods, including our approximate density functional implementation, would likely fail to describe properly the electronic structure of that state. Table 2 shows the T1-diagnostic of the HMXH⁺ intermediates of Equations (2) to (5).

Table 2. The T1-diagnostic values of HMXH⁺ (M = Pd, Pt X = O, S).

	T1-diagnostic		T1-diagnostic
² HPdOH ⁺	0.066	² HPtOH ⁺	0.028
⁴ HPdOH ⁺	0.041	⁴ HPtOH ⁺	0.039
² HPdSH ⁺	0.031	² HPtSH ⁺	0.032
⁴ HPdSH ⁺	0.029	⁴ HPtSH ⁺	0.027

It is observed that only the doublet state of HPdOH⁺ has a T1-diagnostic value larger than the recommended threshold, and that its quartet state lies on the mark. We have recalculated both states with a multiconfigurational CASSCF(17,12) wave function. Notice that the selected active space contains all the valence electrons and all the valence orbitals resulting from the atomic configurations of the Pd 4d⁹ 5s^{0.1}, O 2s²2p⁴ and H 1s¹. We have found that the relative energy between the doublet and quartet states of HPdOH⁺ increases from our 1.41 eV calculated at the CCSD(T)//B3LYP level of theory to 1.48 eV. This does not, however, alter the main features of the reaction path. The main configuration of the doublet state, with a coefficient of 0.481, corresponds to the single configuration of our CCSD(T) calculation. The configuration with second largest coefficient, 0.380, corresponds to the main configuration of the quartet state with doublet coupling. The quartet state is found to be less multiconfigurational in nature than the doublet state, as mentioned above. Thus, the main configuration coefficient is 0.846 and the second largest is 0.344.

The main electronic configuration for both the palladium and platinum compounds are similar. Hence, only the electronic structures of HPdOH⁺ and HPdSH⁺ will be discussed. As shown in Figure 3, the HPdOH⁺, in both lowest energy doublet and quartet states, has two doubly occupied non-bonding 4d orbitals of palladium, namely, 4d_{xy} and

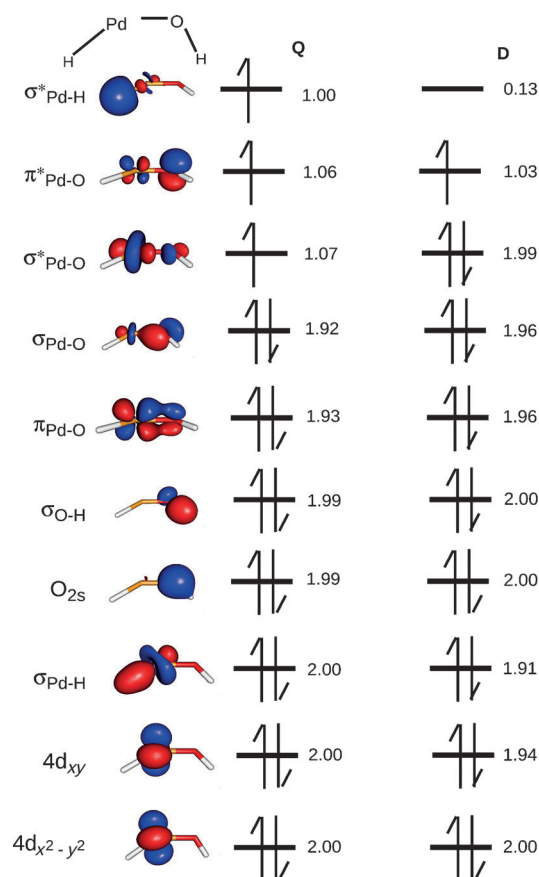


Figure 3. CASSCF(17,12) natural orbitals and their occupation numbers for the quartet (Q) and doublet (D) states of HPdOH⁺.

$4d_{x^2-y^2}$ (given that molecule lies in the xz plane with the z axis along the PdO bond). Both Pd–H and Pd–O σ bonds are formed by using the $4d_{xz}$ and $4d_{z^2}$ orbitals of palladium, respectively. Finally, the Pd–O π bond is formed by the $4d_{yz}$ orbital of palladium. These bonding orbitals are followed by three antibonding orbitals, although it is noteworthy that the Pd–O σ^* antibonding orbital has a large contribution from the $5s$ orbital of Pd. In the doublet state, the Pd–O σ^* antibonding orbital is doubly occupied, and the unpaired electron is located in the π^* antibonding one. Furthermore, in the quartet state, the three unpaired electrons are located in the above mentioned three antibonding orbitals.

On the other hand, for the HPdSH⁺ cation, the $4d_{xy}$, $4d_{x^2-y^2}$ and $4d_{yz}$ orbitals of palladium are non-bonding in both the quartet and doublet states, and remain fully occupied. The Pd–O bonding π and antibonding π^* now become the $4d_{yz}$ orbital of Pd and the $3p_y$ orbital of sulfur in HPdSH⁺, perpendicular to the molecular plane. The Pd–H and Pd–S σ bonds are formed by using both $4d_{xz}$ and $4d_{x^2-y^2}$ orbitals of palladium, respectively. In the doublet state, the Pd–S σ^* antibonding orbital is doubly occupied, the Pd–H σ^* is unoccupied and the single unpaired electron is located in the $3p_y$ orbital of sulfur. In the quartet state, in addition to the singly occupied $3p_y$ orbital of sulfur, the Pd–H and Pd–S σ^* antibonding orbitals are also singly occupied.

Taking into account that the largest coefficients of the antibonding orbitals are those of the palladium orbitals, it is predicted that in the two spin states of both HPdOH⁺ and HPtOH⁺, the palladium and platinum are in Pd^{III} and Pt^{III} formal oxidation states. On the other hand, since the –SH ligand is less electronegative than the –OH ligand, the formal oxidation states of the metals in HPdSH⁺ and HPtSH⁺ are Pd^{II} and Pt^{II}, respectively.

Thus, with these electronic configurations we can say that none of the HMXH⁺ intermediates requires an electron transfer from the metal to the oxygen (or sulfur) to pass from the quartet to the doublet state. In fact, a single electron flip and a following orbital reorganization connects one state to the other.

Electronic Structure of MX⁺ (M=Pd, Pt; X=O, S): The bond dissociation energies of both oxides, PdO⁺ and PtO⁺, and the palladium sulfide, PdS⁺, cations have been measured by Armentrout et al.^[65–67] Additionally, Metz et al.^[64] have also measured the bond dissociation energy of PtO⁺. We are not aware of any thermodynamic measurements of the bond dissociation energy of PtS⁺. Hence, we have conducted large scale CASSCF/CASPT2(13,9) calculations with the ANO-RCC quadruple-zeta basis set, to have reference data to compare our CCSD(T)//B3LYP results. Table 3 shows the harmonic vibrational energies, bond lengths, and the bond dissociation energies calculated at the CCSD(T)//B3LYP, for both the quartet and doublet spin states.

The CASSCF/CASPT2(13,9) dominant valence electronic configuration of the ground quartet $^4\Sigma^-$ state of PtS⁺ is $(1\sigma)^2(2\sigma)^2(1\pi)^4(1\delta)^4(3\sigma^*)^1(2\pi^*)^2$, in which the 1σ orbital corresponds largely to the atomic $3s$ orbital of sulfur, the 2σ and 1π orbitals are the Pt–S bonding orbitals, the 1δ are non-bonding platinum $5d$ orbitals, the $3\sigma^*$ is the platinum

Table 3. Equilibrium bond lengths [\AA], harmonic vibrational frequencies [cm^{-1}], and dissociation energies [eV] of the low-lying quartet and doublet states of the palladium oxide, palladium sulfide, platinum oxide, and platinum sulfide cations at the CCSD(T)//B3LYP level of theory. Experimental bond-dissociation energies are shown in parenthesis. The bond-dissociation energy of PtS⁺ shown in parenthesis has been estimated at CASSCF/CASPT2 level of theory; see the main text for details.

		$^4\Sigma$	$^2\Sigma$
PdO ⁺	R_e	1.782	1.788
	ω_e	692	641
	D_o	1.783	1.296
		(1.46±0.12) ^[65]	
PdS ⁺	R_e	2.141	2.149
	ω_e	391	373
	D_o	2.283	1.993
		(2.36±0.11) ^[67]	
PtO ⁺	R_e	1.732	1.733
	ω_e	821	827
	D_o	3.198	2.891
		(3.26±0.07) ^[66]	
PtS ⁺	R_e	2.096	2.101
	ω_e	466	464
	D_o	3.729	3.522
		(4.27)	

5s atomic orbital, and the 2 π^* degenerate two orbitals are Pt–S antibonding orbitals. The lowest energy doublet is the $^2\Sigma^-$ state, which lies 0.22 eV higher in energy. It has the same dominant valence electronic configuration as the low-lying $^4\Sigma^-$ quartet state, but the 3 σ^* and 2 π^* orbitals are doublet paired.

The dominant valence electronic configurations of the remaining diatoms, PdO⁺, PtO⁺, and PdS⁺, as calculated by Armentrout et al.^[65–67] and ourselves in the present investigation, are entirely analogous to the one described for PtS⁺ above. The minor quantitative differences observed should be ascribed to the different basis sets used.

Inspection of Table 3 shows that the theoretically calculated bond dissociation energies agree well with their corresponding experimental (highly accurate theoretical for PtS⁺) marks. In this sense, it is observed that the greater discrepancy with the experiment corresponds to the dissociation energy of the PdO⁺ diatom, in which the calculations provide with an energy of 1.783 eV compared with the experimental value of (1.46 ± 0.12).^[65] The calculated dissociation energy of PdS⁺ diatom, 2.283 eV, agrees very well with the experimental value (2.36 ± 0.11),^[67] as well as the calculated PtO⁺ dissociation energy, 3.198 eV, with the corresponding experimental value (3.26 ± 0.07).^[66] This confirms the assignment of the ground state to the $^4\Sigma^-$ state.

Additionally, in accordance with the earlier observation of Armentrout et al.,^[67] it is seen that our calculated doublets have slightly longer bond lengths and slightly smaller harmonic vibrational frequencies than their corresponding quartet states.

Finally, it is worth noticing that platinum forms stronger bonds than palladium with both oxygen and sulfur. Therefore, after an initial decrease of the bond dissociation energy for Ni to Pd, as a result of the relativistic contraction, it increases when moving down to Pt in the periodic table.

Conclusions

In accordance with our calculations, we propose that the reactions of palladium and platinum cations with water and hydrogen sulfide proceed by the successive migrations of the two hydrogen atoms over the metal center, at which a H–H bond develops to form a complex between the hydrogen molecule and the metal sulfide or metal oxide cation. From these intermediates the loss of H₂ proceeds without a transition state to the corresponding products. Although the energetic parameters depend on the reaction studied, we have found that, whereas both reactions of the palladium occur with two transition states, in the reactions of platinum a third transition state is needed to obtain the final products. In these cases, the second transition state leads to the formation of a dihydrido Kubas-like complex, namely XPt(H)(H)⁺ (X = O, S) and, through TS3, both hydrogen atoms approach each other, forming the H–H bond.

For all the reactions studied, we have found that one crossing between the doublet and quartet states potential

energy surfaces occurs. This spin-crossing takes place around the last transition state, yielding a H₂MX⁺ intermediate with a quartet ground state.

We have found that the ground state of the HMXH⁺ intermediate of the four reactions is the doublet spin state, and that the quartet state lies between 1.30 and 1.90 eV above. The study of the molecular orbitals of their corresponding main valence electronic configurations reveals that, in contrast with the HNiOH⁺ but along with HNiSH⁺, they have their doublet and quartet spin states connected by a single electron flip. Furthermore, we have found that, except for the HPdSH⁺, the energy barrier associated with the HMXH⁺/MXH₂⁺ isomerization is large enough that the HMXH⁺ should have a long enough lifetime to react with other small molecules like methane.

Acknowledgements

This research was funded by Eusko Jaurilaritza (the Basque Government) Grant IT588-13, and the Spanish Office for Scientific Research, Grant CTQ2011-27374. Likewise, O.L. would like to thank the Government of Navarre for a grant (CTQ2011-27374). J.M.M. would like to thank the Spanish Ministry of Science and Innovation for funding through a Ramón y Cajal Fellowship (RyC 2008-03216). The SGI/IZO-SGIker UPV/EHU (supported by Fondo Social Europeo and MCyT) is gratefully acknowledged for generous allocation of computational resources. P.B.A. acknowledges support from the National Science Foundation, Grant CHE-1049580.

- [1] P. B. Armentrout, *Science* **1991**, *251*, 175–179.
- [2] H. Schwarz, *Angew. Chem.* **2011**, *123*, 10276–10297; *Angew. Chem. Int. Ed.* **2011**, *50*, 10096–10115.
- [3] A. Bozović, S. Feil, G. K. Koyanagi, A. A. Viggiano, X. Zhang, M. Schlängen, H. Schwarz, D. K. Bohme, *Chem. Eur. J.* **2010**, *16*, 11605–11610.
- [4] J. Roithová, D. Schröder, *Chem. Rev.* **2010**, *110*, 1170–1211.
- [5] K. J. de Almeida, H. A. Duarte, *Organometallics* **2009**, *28*, 3203–3211.
- [6] R. N. Perutz, S. Sabo-Etienne, *Angew. Chem.* **2007**, *119*, 2630–2645; *Angew. Chem. Int. Ed.* **2007**, *46*, 2578–2592.
- [7] O. Mó, M. Yáñez, J. Y. Salpin, J. Tortajada, *Mass Spectrom. Rev.* **2007**, *26*, 474–516.
- [8] A. Shayesteh, V. V. Lavrov, G. K. Koyanagi, D. K. Bohme, *J. Phys. Chem. A* **2009**, *113*, 5602–5611.
- [9] D. Schröder, H. Schwarz, *Proc. Natl. Acad. Sci. USA* **2008**, *105*, 18114–18119.
- [10] B. A. Vastine, M. B. Hall, *J. Am. Chem. Soc.* **2007**, *129*, 12068–12069.
- [11] P. B. Armentrout, *J. Phys. Chem. A* **2006**, *110*, 8327–8338.
- [12] O. Lakuntza, J. M. Matxain, J. M. Ugalde, *ChemPhysChem* **2010**, *11*, 3172–3178.
- [13] S. Chiodo, O. Kondakova, M. C. Michellini, N. Russo, E. Sicilia, A. Irigoras, J. M. Ugalde, *J. Phys. Chem. A* **2004**, *108*, 1069–1081.
- [14] Y. Wang, Q. Wang, Z. Geng, L. Lv, Y. Si, Q. Wang, H. Liu, D. Cui, *J. Phys. Chem. A* **2009**, *113*, 13808–13815.
- [15] R. Kretschmer, M. Schlängen, H. Schwarz, *Chem. Eur. J.* **2012**, *18*, 40–49.
- [16] S. J. Dee, V. A. Castleberry, O. J. Villarroel, I. E. Laboren, D. J. Bellet, *J. Phys. Chem. A* **2010**, *114*, 1783–1789.
- [17] D. E. Clemmer, N. Aristov, P. B. Armentrout, *J. Phys. Chem.* **1993**, *97*, 544–552.
- [18] D. E. Clemmer, Y. M. Chen, F. A. Khan, P. B. Armentrout, *J. Phys. Chem.* **1994**, *98*, 6522–6529.

- [19] Y. M. Chen, D. E. Clemmer, P. B. Armentrout, *J. Phys. Chem.* **1994**, 98, 11490–11498.
- [20] P. Cheng, G. K. Koyanagi, D. K. Bohme, *J. Phys. Chem. A* **2007**, 111, 8561–8573.
- [21] A. Irigoras, J. E. Fowler, J. M. Ugalde, *J. Phys. Chem. A* **1998**, 102, 293–300.
- [22] A. Irigoras, J. E. Fowler, J. M. Ugalde, *J. Am. Chem. Soc.* **1999**, 121, 574–580.
- [23] N. Russo, E. Sicilia, *J. Am. Chem. Soc.* **2001**, 123, 2588–2596.
- [24] A. Irigoras, J. E. Fowler, J. M. Ugalde, *J. Am. Chem. Soc.* **1999**, 121, 8549–8558.
- [25] M. C. Michelini, E. Sicilia, N. Russo, *J. Phys. Chem. A* **2003**, 107, 4862–4868.
- [26] A. Irigoras, O. Elizalde, I. Silanes, J. E. Fowler, J. M. Ugalde, *J. Am. Chem. Soc.* **2000**, 122, 114–122.
- [27] M. Schlangen, D. Schröder, H. Schwarz, *Angew. Chem.* **2007**, 119, 1667–1671; *Angew. Chem. Int. Ed.* **2007**, 46, 1641–1644.
- [28] Y. Dede, X. Zhang, M. Schlangen, H. Schwarz, M.-H. Baik, *J. Am. Chem. Soc.* **2009**, 131, 12634–12642.
- [29] X. Zhang, M. Schlangen, M.-H. Baik, Y. Dede, H. Schwarz, *Helv. Chim. Acta* **2009**, 92, 151–164.
- [30] P. E. M. Siegbahn, M. R. A. Blomberg, H. Svensson, *J. Phys. Chem.* **1993**, 97, 2564–2570.
- [31] M. C. del Carmen Michelini, N. Russo, E. Sicilia, *Angew. Chem.* **2006**, 118, 1113–1117; *Angew. Chem. Int. Ed.* **2006**, 45, 1095–1099.
- [32] G. C. Bond, *J. Mol. Catal. A: Chem.* **2000**, 156, 1–20.
- [33] C. Heinemann, H. Schwarz, W. Koch, K. G. Dyall, *J. Chem. Phys.* **1996**, 104, 4642–4652.
- [34] G. T. de Jong, A. Kovács, F. M. Bickelhaupt, *J. Phys. Chem. A* **2006**, 110, 7943–7951.
- [35] A. Diefenbach, F. M. Bickelhaupt, *J. Chem. Phys.* **2001**, 115, 4030–4041.
- [36] H. Zhang, K. Balasubramanian, *J. Phys. Chem.* **1992**, 96, 6981–6985.
- [37] J. N. Harvey, M. Aschi, *Faraday Discuss.* **2003**, 124, 129–143.
- [38] Gaussian 09, Revision A.02, M. J. Frisch, G. W. Trucks, H. B. Schlegel, G. E. Scuseria, M. A. Robb, J. R. Cheeseman, G. Scalmani, V. Barone, B. Mennucci, G. A. Petersson, H. Nakatsuji, M. Caricato, X. Li, H. P. Hratchian, A. F. Izmaylov, J. Bloino, G. Zheng, J. L. Sonnenberg, M. Hada, M. Ehara, K. Toyota, R. Fukuda, J. Hasegawa, M. Ishida, T. Nakajima, Y. Honda, O. Kitao, H. Nakai, T. Vreven, J. A. Montgomery, Jr., J. E. Peralta, F. Ogliaro, M. Bearpark, J. J. Heyd, E. Brothers, K. N. Kudin, V. N. Staroverov, R. Kobayashi, J. Normand, K. Raghavachari, A. Rendell, J. C. Burant, S. S. Iyengar, J. Tomasi, M. Cossi, N. Rega, J. M. Millam, M. Klene, J. E. Knox, J. B. Cross, V. Bakken, C. Adamo, J. Jaramillo, R. Gomperts, R. E. Stratmann, O. Yazyev, A. J. Austin, R. Cammi, C. Pomelli, J. W. Ochterski, R. L. Martin, K. Morokuma, V. G. Zakrzewski, G. A. Voth, P. Salvador, J. J. Dannenberg, S. Dapprich, A. D. Daniels, O. Farkas, J. B. Foresman, J. V. Ortiz, J. Cioslowski, D. J. Fox, Gaussian, Inc., Wallingford, CT, **2009**.
- [39] ADF, Amsterdam Density Functional program, Theoretical Chemistry, Vrije Universiteit Amsterdam, URL: <http://www.scm.com>, **2007**.
- [40] A. D. Becke, *Phys. Rev. A* **1988**, 38, 3098–3100.
- [41] A. D. Becke, *J. Chem. Phys.* **1993**, 98, 5648–5653.
- [42] C. Lee, W. Yang, R. G. Parr, *Phys. Rev. B* **1988**, 37, 785–789.
- [43] P. Hohenberg, W. Kohn, *Phys. Rev.* **1964**, 136, B864–B871.
- [44] W. Kohn, L. J. Sham, *Phys. Rev.* **1965**, 140, A1133–A1138.
- [45] K. A. Peterson, D. Figgen, M. Dolg, H. Stoll, *J. Chem. Phys.* **2007**, 126, 124101.
- [46] D. Figgen, K. Peterson, M. Dolg, H. Stoll, *J. Chem. Phys.* **2009**, 130, 164108.
- [47] J. S. Krishnan, J. S. Binkley, D. Seeger, J. A. Pople, *J. Chem. Phys.* **1980**, 72, 650–655.
- [48] C. Adamo, V. Varone, *J. Chem. Phys.* **1999**, 110, 6158–6171.
- [49] S. Faas, J. G. Snijders, J. H. van Lenthe, E. van Lenthe, E. J. Baerends, *Chem. Phys. Lett.* **1995**, 246, 632–640.
- [50] C. Chang, N. Pelissier, P. Durand, *Phys. Scr.* **1986**, 34, 394–404.
- [51] J. M. Mercero, J. M. Matxain, X. Lopez, D. M. York, A. Largo, L. A. Eriksson, J. M. Ugalde, *Int. J. Mass Spectrom.* **2005**, 240, 37–99.
- [52] J. A. Pople, R. Krishnan, H. B. Schlegel, J. S. Binkley, *Int. J. Quant. Chem.* **1978**, 14, 545–560.
- [53] R. J. Bartlett, G. D. Purvis, *Int. J. Quant. Chem.* **1978**, 14, 561–581.
- [54] B. O. Roos, R. Lindh, P.-Å. Malmqvist, V. Veryazov, P.-O. Widmark, *J. Phys. Chem. A* **2005**, 109, 6575–6579.
- [55] B. O. Roos, R. Lindh, P.-Å. Malmqvist, V. Veryazov, P.-O. Widmark, *J. Phys. Chem. A* **2004**, 108, 2851–2858.
- [56] P.-O. Widmark, P.-Å. Malmqvist, B. O. Roos, *Theor. Chim. Acta* **1990**, 77, 291–306.
- [57] F. Aquilante, L. De Vico, N. Ferré, G. Ghigo, P.-Å. Malmqvist, P. Neogrády, T. B. Pedersen, M. Pitoňák, M. Reiher, B. O. Roos, L. Serrano-Andrés, M. Urban, V. Veryazov, R. Lindh, *J. Comput. Chem.* **2010**, 31, 224–247.
- [58] D. Schröder, S. Shaik, H. Schwarz, *Acc. Chem. Res.* **2000**, 33, 139–145.
- [59] N. F. Dalleska, K. Honma, L. S. Sunderlin, P. B. Armentrout, *J. Am. Chem. Soc.* **1994**, 116, 3519–3528.
- [60] T. J. Lee, P. R. Taylor, *Int. J. Quantum Chem. Quant. Chem. Symp.* **1989**, S23, 199–207.
- [61] P. R. Taylor, *Lecture Notes in Quantum Chemistry II*, Vol. 64, Springer, Berlin, **1994**, 125–202.
- [62] M. Diefenbach, H. Schwarz, *Chem. Eur. J.* **2005**, 11, 3058–3063.
- [63] C. J. Thompson, K. L. Stringer, M. McWilliams, R. B. Metz, *Chem. Phys. Lett.* **2003**, 376, 588–594.
- [64] Y.-M. Chen, P. B. Armentrout, *J. Chem. Phys.* **1995**, 103, 618–626.
- [65] X.-G. Zhang, P. B. Armentrout, *J. Phys. Chem. A* **2003**, 107, 8904–8914.
- [66] P. B. Armentrout, I. Kretzschmar, *Inorg. Chem.* **2009**, 48, 10371.
- [67] Y. Ralchenko, A. Kramida, J. Reader, NIST ASD Team (2012), NIST Atomic Spectra Database, Version 5.0; available at <http://physics.nist.gov/asd3> (2012, December 5), National Institute of Standards and Technology, Gaithersburg, MD.

Received: January 21, 2013

Revised: March 7, 2013

Published online: May 22, 2013